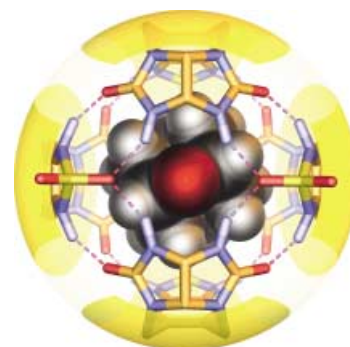


COVER PICTURE

The cover picture shows adamantane-2,6-dione encapsulated within a hydrogen-bonded capsule made up of four identical subunits. The ketone functionality of the guest molecule (CPK model, red) participates in the structural seam at each end of the capsule through bifurcated hydrogen bonds. Find out more about encapsulating complexes in the review by Rebek, Jr., et al. on p. 1488 ff.

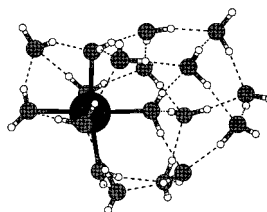


REVIEWS

Contents

Cluster structures, predictably unpredictable?

Theoretical determination of cluster structures is difficult for various reasons. Problems are posed not only by the size of the cluster and the extremely large number of local energy minima induced by its size, but also by the discontinuous dependence of basic structural principles on size, which is noticed empirically again and again. This situation can lead to structures that are intuitively hard to understand, for example, in the case of microhydration clusters of the sodium cation (see picture). An exemplary overview of current work demonstrates that we are still far away from a basic understanding of these structural transitions.



B. Hartke * 1468–1487

Structural Transitions in Clusters

Keywords: aggregation • cluster compounds • global optimization • magic numbers • structure elucidation

Angew. Chem. **2002**, *114*, 1534–1554

The medium is the message: Molecules encapsulated within noncovalent host frameworks (see picture) are reversibly isolated from the influence of solvent molecules and other reagents at room temperature and in solution. These complexes give rise to a wide variety of emergent properties including chiral selection, transduction of optical signals, polymerization, catalysis, and the stabilization of reactive species.

Angew. Chem. **2002**, *114*, 1556–1578



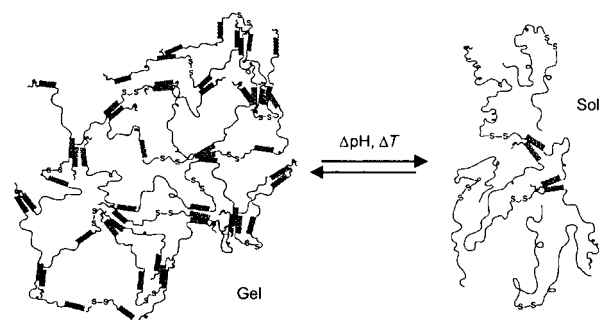
F. Hof, S. L. Craig, C. Nuckolls,
J. Rebek, Jr. * 1488–1508

Molecular Encapsulation

Keywords: host–guest systems •
molecular capsules • molecular
recognition • self-assembly

HIGHLIGHTS

Absolute uniform chain lengths and amino acid sequences as well as well-defined folding patterns that determine structure and properties characterize natural proteins. Advances in chemical and biological peptide synthesis allow improved control over the composition and structure of artificial proteins and peptide hybrid materials, which opens up pathways for the development of new protein-inspired materials, for example, reversible protein hydrogels (see scheme).



Angew. Chem. **2002**, *114*, 1579–1583

H.-A. Klok * 1509–1513

Protein-Inspired Materials: Synthetic
Concepts and Potential Applications

Keywords: biosynthesis • peptides •
proteins • ring-opening polymerization •
solid-phase synthesis

VIPs

The following communications are “Very Important Papers” in the opinion of two referees. They will be published shortly (those marked with a diamond will be published in the next issue). Short summaries of these articles can be found on the *Angewandte Chemie* homepage at the address <http://www.angewandte.com>

Synthesis and Structure of Na_3N

D. Fischer, M. Jansen* ◆

Synthesis and Characterization of a Digermanium Analogue of an Alkyne

M. Stender, A. D. Phillips,
R. J. Wright, P. P. Power* ◆

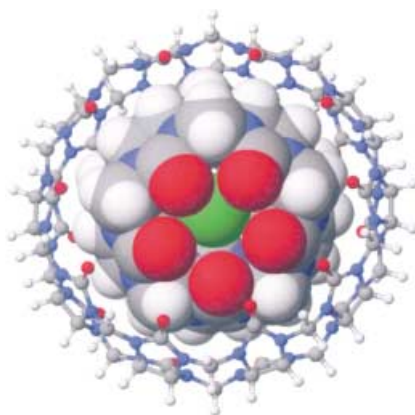
A Short Synthesis of (+)-13-Deoxyserratine

J. Cassayre, F. Gagosz,
S. Z. Zard* ◆

Catalytic Activity and Poisoning of Specific Sites on Supported Metal Nanoparticles

J. Hoffmann, V. Johánek,
J. Hartmann, J. Libuda,*
H.-J. Freund

A spinner in a cage, or put simply, a gyroscope. A “molecular gyroscope”, known as gyroscane (see picture), was recently synthesized. Often such systems are referred to as molecular machines—why not as molecular toys? In this contribution the author illustrates that this view does not have to have negative connotations.



Angew. Chem. **2002**, *114*, 1583–1586

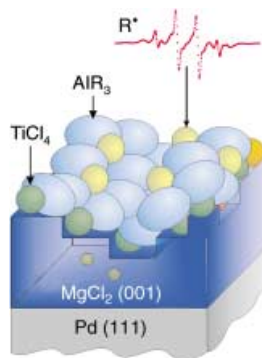
C. A. Schalley* 1513–1515

Of Molecular Gyroscopes, Matroshka Dolls, and Other “Nano”-Toys

Keywords: cucurbituril • host–guest systems • molecular devices • supramolecular chemistry

COMMUNICATIONS

Are radicals involved in the activation of a heterogeneous Ziegler–Natta catalyst? The activation of titanium centers in an active Ziegler–Natta model system initiated by alkyl aluminum compounds has been shown by ESR spectroscopy under ultrahigh-vacuum conditions to proceed, in the case of trimethylaluminum, by a radical mechanism (see picture). In contrast, no indication of radical production is found when the ethyl derivative is used for activation.



Angew. Chem. **2002**, *114*, 1587–1591

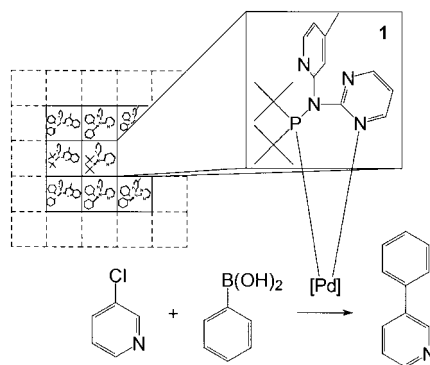
T. Risse,* J. Schmidt, H. Hamann, H.-J. Freund 1517–1520

Direct Observation of Radicals in the Activation of Ziegler–Natta Catalysts

Keywords: EPR spectroscopy • heterogeneous catalysis • surface chemistry • Ziegler–Natta catalysts



The parallel synthesis of homogeneous catalysts is successful with ligands such as **1**. They coordinate metals of Group 10 with the formation of a five-membered chelate ring (see scheme). The resulting metal complexes are efficient catalysts which can activate C(aryl)–chloro bonds and can, for example, mediate the Suzuki coupling of 3-chloropyridine with phenylboronic acid to form 3-phenylpyridine.



Angew. Chem. **2002**, *114*, 1591–1594

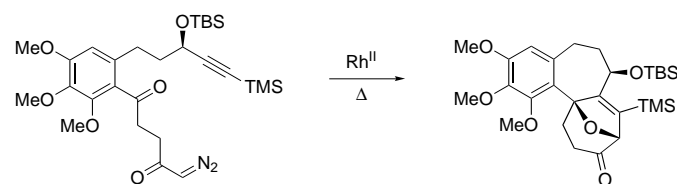
T. Schareina, R. Kempe* ... 1521–1523

Combinatorial Libraries with P-Functionalized Aminopyridines: Ligands for the Preparation of Efficient C(Aryl)–Cl Activation Catalysts

Keywords: C–C coupling • C–Cl activation • chelates • combinatorial chemistry • N,P ligands



The major alkaloid of the meadow saffron is colchicine, which displays remarkable antimitotic activity and has long been used in the treatment of acute gout and is currently being tested against a broad variety of other diseases. In a remarkable Rh-catalyzed domino transformation, the complete carbon skeleton of this important alkaloid is assembled with high efficiency (see scheme). TBS = *tert*-butyldimethylsilyl, TMS = trimethylsilyl.



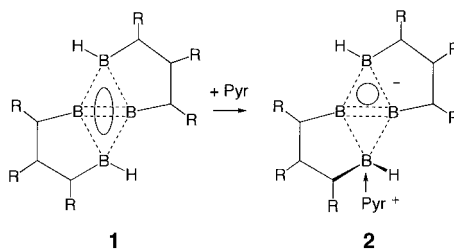
Angew. Chem. **2002**, *114*, 1594–1597

T. Graening, W. Friedrichsen, J. Lex, H.-G. Schmalz* 1524–1526

Facile Construction of the Colchicine Skeleton By a Rhodium-Catalyzed Cyclization/Cycloaddition Cascade

Keywords: alkaloids • cycloaddition • polycycles • rhodium • ylides

The diamond-shaped tetraborane(6) **1** and its pyridine adduct **2** are the first aromatic compounds in which two π electrons display cyclic delocalization over four and three boron centers, respectively (see scheme). The two compounds contain the shortest B–B distances ever observed. R = SiMe₃, Pyr = 4-*tert*-butylpyridine.



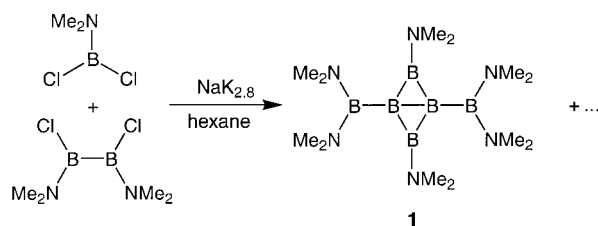
C. Präsang, M. Hofmann, G. Geiseler, W. Massa, A. Berndt * 1526–1529

Aromatic Boranes with Planar-Tetracoordinate Boron Atoms and Very Short B–B Distances

Keywords: aromaticity • boron • density functional calculations • electronic structure • multicenter bonds

Angew. Chem. **2002**, *114*, 1597–1599

The reduction of dimethylaminodichloroborane and dimethylaminodichlorodiborane(4) with NaK_{2.8} alloy provides the new tetraborane(4) **1** (see scheme). The unusual bonding situation in **1** is explained on the basis of molecular-orbital calculations.



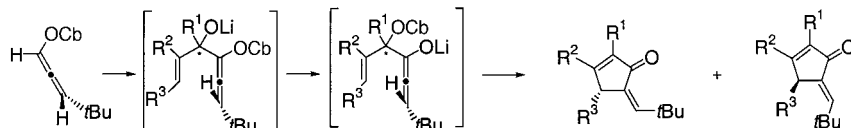
A. Maier, M. Hofmann, H. Pritzkow, W. Siebert * 1529–1532

A Planar, Aromatic *bicyclo*-Tetraborane(4)

Keywords: aromaticity • boron • density functional calculations • electronic structure • multicenter bonds

Angew. Chem. **2002**, *114*, 1600–1602

A stereospecific ring-closure reaction takes place between chiral allenyl carbamates and enones. After lithiation, carbonyl addition, and subsequent carbamoyl (Cb = CONiPr₂) group migration (see scheme), a stereospecific conrotatory cyclization leads to 5-alkylidene-2-cyclopentenones.



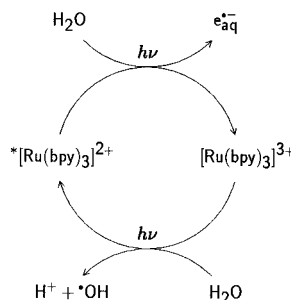
C. Schultz-Fademrecht, M. A. Tius,* S. Grimme,* B. Wibbeling, D. Hoppe * 1532–1535

Synthesis of Enantioenriched 5-Alkylidene-2-cyclopentenones from Chiral Allenyl Carbamates: Generation of a Chiral Lithium Allenolate and Allylic Activation for a Conrotatory 4 π -Electrocyclization

Keywords: allenes • asymmetric synthesis • chirality transfer • cyclization • cyclopentenones

Angew. Chem. **2002**, *114*, 1610–1612

In spite of its model character, the mechanism of the photoionization described here has received very little attention. It is demonstrated that the electronically excited species $^*[Ru(bpy)_3]^{2+}$ acts as a catalyst, and is regenerated in its excited state by a photoreaction of the ionized ruthenium complex $[Ru(bpy)_3]^{3+}$ with water (see catalytic cycle; bpy = 2,2'-bipyridine).



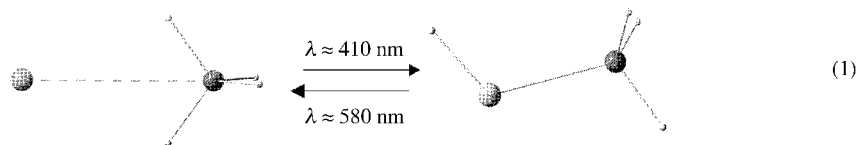
M. Goez,* M. Schiewek, M. H. O. Musa 1535–1538

Near-UV Photoionization of $[Ru(bpy)_3]^{2+}$: A Catalytic Cycle with an Excited Species as Catalyst

Keywords: kinetics • laser chemistry • photochemistry • ruthenium • solvated electrons

Angew. Chem. **2002**, *114*, 1606–1609

Matrix isolation experiments have enabled the first characterization of the aluminum–silane complex $\text{Al} \cdot \text{SiH}_4$ (η^2 coordination) which can be converted reversibly by selective photolysis into its tautomer HAlSiH_3 [Eq. (1)]. Broadband UV/Vis photolysis causes decomposition of HAlSiH_3 to give the aluminum(I) species AlSiH_3 .



Angew. Chem. **2002**, *114*, 1602–1606

B. Gaertner, H.-J. Himmel* . 1538–1541

Characterization and Photochemistry of the Silane–Aluminum Complex $\text{Al} \cdot \text{SiH}_4$ and Its Photoproducts HAlSiH_3 and AlSiH_3 in a Solid Argon Matrix

Keywords: aluminum • insertion • matrix isolation • photolysis • silane

In situ ultrasmall-angle X-ray scattering (USAXS) on polymer- and protein-mediated silica transformations revealed a phase-separation process in which mesophases direct silica aggregation. The USAXS spectra obtained from the synthesized silica have characteristic features that resemble those observed for pore structures in diatom exoskeletons. The hypothesis that mesophases could explain silica biomineralization in diatoms is discussed.

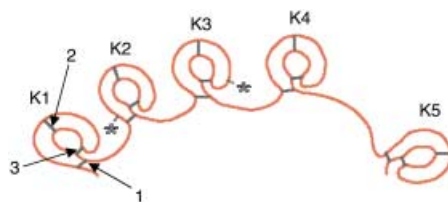
Angew. Chem. **2002**, *114*, 1613–1616

E. G. Vrieling,* T. P. M. Beelen,
R. A. van Santen,
W. W. C. Gieskes* 1543–1546

Mesophases of (Bio)Polymer–Silica Particles Inspire a Model for Silica Biomineralization in Diatoms

Keywords: bioinorganic chemistry • biomineralization • diatoms • silicon • ultrasmall-angle X-ray scattering

The redox environment controls the topology and mechanical properties of angiotensin by modifying the extent of pairing of the three internal disulfide bonds (1–3, see picture) within its five Kringle domains (K1–K5). This situation was revealed by single-molecule force-spectroscopy experiments, analysis of the data, which also allowed the distribution of the different thiol/disulfide reduction intermediates to be estimated.




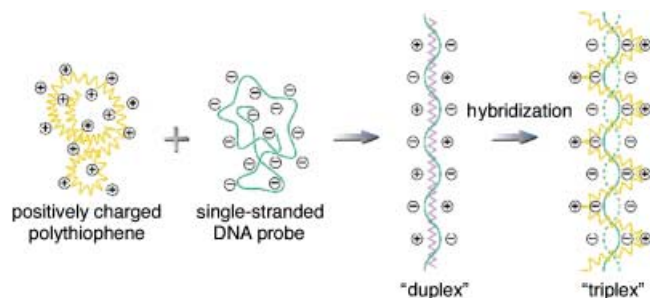
Angew. Chem. **2002**, *114*, 1616–1618

Y. Bustanji, B. Samori* 1546–1548

The Mechanical Properties of Human Angiotensin Can Be Modulated by Means of Its Disulfide Bonds: A Single-Molecule Force-Spectroscopy Study

Keywords: proteins • reduction • scanning probe microscopy • single-molecule studies

 **Different electrostatic interactions** and conformational structures between single- or double-stranded negatively charged nucleic acids bound to a surface (see picture) and water-soluble cationic poly(3-alkoxy-4-methylthiophene) derivatives (in yellow) provide the basis for a sensitive optical detection method (colorimetric or fluorometric) for oligonucleotide hybridization.



Angew. Chem. **2002**, *114*, 1618–1621

H.-A. Ho, M. Boissinot, M. G. Bergeron,
G. Corbeil, K. Doré, D. Boudreau,
M. Leclerc* 1548–1551

Colorimetric and Fluorometric Detection of Nucleic Acids Using Cationic Polythiophene Derivatives

Keywords: conducting materials • DNA recognition • electrostatic interactions • fluorescence • nucleic acids • sensors

A simple yet powerful strategy for the molecular design of chiral phase-transfer catalysts: Conformationally flexible, *N*-spiro chiral quaternary ammonium bromides of type **1** have been newly designed and are found to exert high chiral efficiency by taking advantage of the considerable difference of activity between the diastereomeric homo- and heterochiral isomers through rapid conformational interconversion.



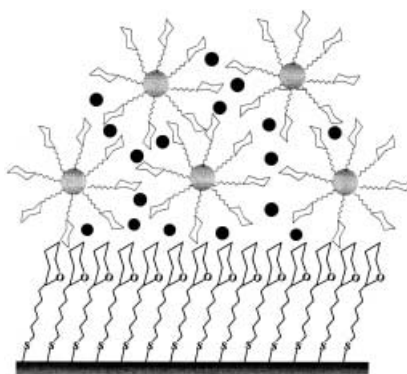
Angew. Chem. **2002**, *114*, 1621–1624

T. Ooi, Y. Uematsu, M. Kameda,
K. Maruoka* 1551–1554

Conformationally Flexible, Chiral
Quaternary Ammonium Bromides for
Asymmetric Phase-Transfer Catalysis

Keywords: alkylation • asymmetric
catalysis • atropinversion •
conformational flexibility • phase-
transfer catalysis

More evidence for carbohydrate self-interactions as a first step in cell adhesion and recognition has been found in experiments with gold glyconanoparticles and self-assembled monolayers presenting carbohydrate epitopes (see picture). The Ca^{2+} -ion-dependent interactions were studied and quantified by surface plasmon resonance. Gray circles = gold nanoparticles, black circles = Ca^{2+} ions.



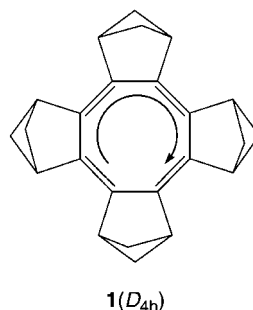
Angew. Chem. **2002**, *114*, 1624–1627

M. J. Hernáiz, J. M. de la Fuente,
Á. G. Barrientos,
S. Penadés* 1554–1557

A Model System Mimicking
Glycosphingolipid Clusters to Quantify
Carbohydrate Self-Interactions by
Surface Plasmon Resonance

Keywords: carbohydrates • glycolipids •
noncovalent interactions • self-assembly •
surface plasmon resonance

Despite considerable bond alternation, the planar cyclooctatetraene (COT) moiety in tetrakis(bicyclo[2.1.1]hexeno)cyclooctatetraene (**1**(D_{4h})) sustains a strong central paratropic ring current, as expected of an antiaromatic monocycle. The paratropic ring current of the COT moiety can be switched on or off by tuning the rotationally allowed COT HOMO–LUMO transition, for example, by choosing saturated or unsaturated clamps.



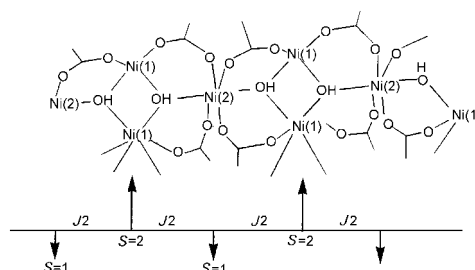
Angew. Chem. **2002**, *114*, 1628–1630

P. W. Fowler, R. W. A. Havenith,
L. W. Jenneskens,* A. Soncini,
E. Steiner 1558–1560

Paratropic Delocalized Ring Currents in
Flattened Cyclooctatetraene Systems with
Bond Alternation

Keywords: ab initio calculations •
annulenes • aromaticity • NMR
spectroscopy • ring currents

Chains of fused Ni^{II} octahedral units form a 3D network and thereby the first example of a homometallic 3D ferrimagnet. The material was characterized by X-ray analysis and a low-temperature magnetic study. The structure features an infinite $\text{Ni}-(\mu_3\text{-OH})\text{-Ni}_2$ -chain and the spin of adjacent Ni centers alternates between $S=1$ and $S=2$ (see picture).



Angew. Chem. **2002**, *114*, 1631–1633

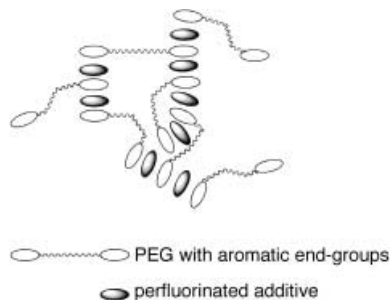
S. Konar, P. S. Mukherjee, E. Zangrando,
F. Lloret,* N. R. Chaudhuri* 1561–1563

A Three-Dimensional Homometallic
Molecular Ferrimagnet

Keywords: coordination chemistry •
ferrimagnetism • magnetic properties •
nickel • O ligands



Stiff PEGs: Aqueous solutions of pyrene end-capped poly(ethylene glycol)s (PEGs) increase their viscosity in the presence of octafluoronaphthalene possibly as a result of aggregation by face-to-face stacking (shown schematically). The exploitation of the arene–perfluoroarene supramolecular synthon in solution is reported.



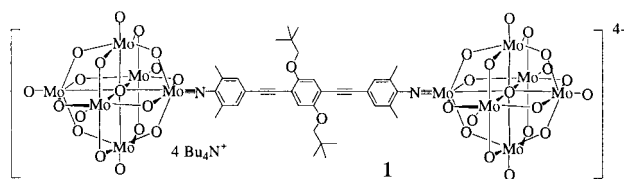
Angew. Chem. **2002**, *114*, 1633–1636

A. F. M. Kilbinger,
R. H. Grubbs* 1563–1566

Arene–Perfluoroarene Interactions as
Physical Cross-Links for Hydrogel
Formation

Keywords: aggregation • gels •
noncovalent interactions • polymers •
stacking interactions

Strong electronic interactions occur between the polyoxometalate (POM) clusters and the π electrons of the conjugated organic bridge in hybrid molecular dumbbells such as **1** which were synthesized by Pd-catalyzed coupling reactions of organoimido-substituted POMs.



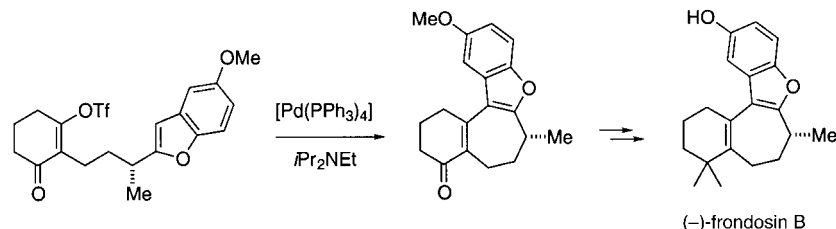
Angew. Chem. **2002**, *114*, 1636–1638

M. Lu, Y. Wei, B. Xu, C. F.-C. Cheung,
Z. Peng,* D. R. Powell 1566–1568

Hybrid Molecular Dumbbells: Bridging
Polyoxometalate Clusters with an Organic
 π -Conjugated Rod

Keywords: C–C coupling •
molybdenum • organic–inorganic hybrid
composites • palladium •
polyoxometalates

Sidestepping stereochemical inversion: In an expedient, asymmetric total synthesis of (–)-frondosin B a novel palladium-catalyzed cyclization establishes the tetracyclic skeleton (see scheme). The absolute stereochemistry of naturally occurring marine metabolite (+)-frondosin B, an interleukin-8 inhibitor, has been reassigned. Tf = trifluoromethanesulfonyl.



Angew. Chem. **2002**, *114*, 1639–1642

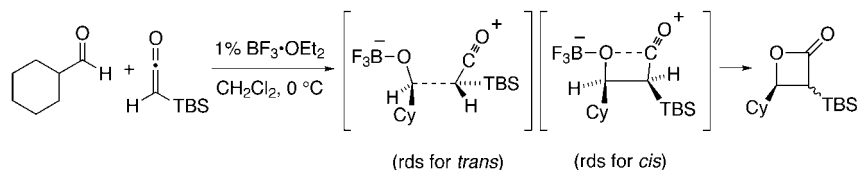
C. C. Hughes, D. Trauner* .. 1569–1572

Concise Total Synthesis of
(–)-Frondosin B Using a Novel
Palladium-Catalyzed Cyclization

Keywords: cyclization • natural
products • palladium • polycycles •
total synthesis



Divergent rate-limiting steps for the formation of diastereomeric products! Evidence for this unexpected finding comes from experimental and theoretical studies of the title reaction. The predicted differing rate-determining steps (rds) in the formation of *cis*- and *trans*- β -lactones (see scheme; cy = cyclohexyl, TBS = *tert*-butyldimethylsilyl) are used to explain the stereoselectivity of these reactions and suggest that a broader range of mechanistic possibilities should sometimes be considered in reactions leading to diastereomeric products.



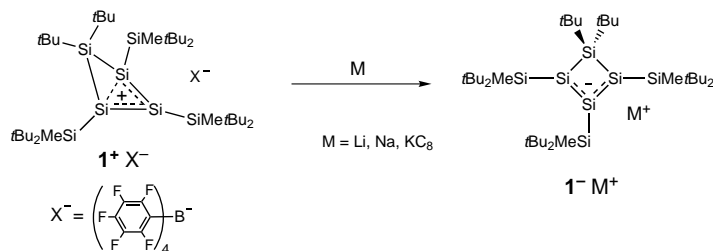
Angew. Chem. **2002**, *114*, 1642–1645

D. A. Singleton,* Y. Wang, H. W. Yang,
D. Romo* 1572–1575

Mechanism and Origin of
Stereoselectivity in Lewis Acid Catalyzed
[2 + 2] Cycloadditions of Ketenes with
Aldehydes

Keywords: ab initio calculations •
cycloaddition • isotope effects •
ketenes • lactones

Alkali-metal derivatives of cyclotetrasilene (1^-) were obtained by the treatment of cyclotetrasilenylium ion (1^+) or cyclotetrasilenyl radical (1^\bullet) with Li, Na, and KC_8 in diethyl ether. X-ray crystallographic analysis of $1^- Li^+$ suggests that it has a cyclotetrasilene structure with a Si=Si bond in the ring, and that the lithium cation interacts with the three silicon atoms in the four-membered-ring skeleton. The ion 1^- is readily oxidized to 1^\bullet and 1^+ ; this is a reversible chemical redox system.



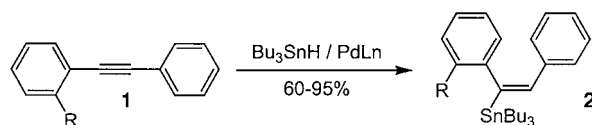
Angew. Chem. **2002**, *114*, 1645–1647

T. Matsuno, M. Ichinohe,
A. Sekiguchi* 1575–1577

Cyclotetrasilene Anion: A Reversible
Redox System of Cyclotetrasilenylium
Cation, Radical, and Anion

Keywords: alkali metals • lithium • redox
chemistry • silicon • small-ring systems

An unprecedented ortho-directing effect (ODE) in diaryl alkynes **1** (R = electron-withdrawing or electron-donating group) promotes regioselective addition of tributyltin hydride to the triple bond and afforded efficiently stannylated unsymmetrical 1,2-diaryl olefins **2**. The precise contributions of steric, electronic, and coordinative factors, which control this regioselectivity are highlighted. The results are rationalized in terms of electronic polarization across the alkyne bond, induced by the *ortho* substituent whatever its electronic nature.



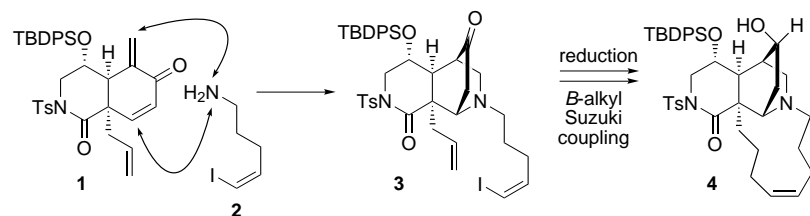
Angew. Chem. **2002**, *114*, 1648–1650

M. Alami,* F. Liron, M. Gervais,
J.-F. Peyrat, J.-D. Brion 1578–1580

Ortho Substituents Direct Regioselective
Addition of Tributyltin Hydride to
Unsymmetrical Diaryl (or Heteroaryl)
Alkynes: An Efficient Route to
Stannylated Stilbene Derivatives

Keywords: alkenes • alkynes •
hydrostannation • palladium • tin

A double Michael addition of amine **2** to **1** was a key reaction in the synthesis of the isoquinuclidine core **4** of xestocyclamine A, a protein kinase C inhibitor. The first ansa bridge was formed efficiently by a *B*-alkyl Suzuki coupling in **3**. TBDPS = *tert*-butyldiphenylsilyl; Ts = *p*-toluenesulfonyl.



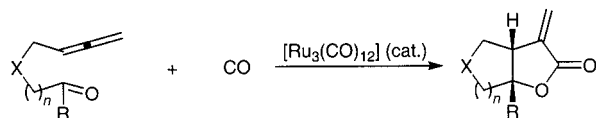
Angew. Chem. **2002**, *114*, 1651–1654

A. Gagnon,
S. J. Danishefsky* 1581–1584

Evaluation of Diene Hierarchies for
Diels–Alder Reactions En Route to
Xestocyclamine A: Elaboration of an
Ansa Bridge by *B*-Alkyl Suzuki
Macrocyclization

Keywords: alkaloids • annulation • cross-
coupling • cycloaddition • macrocycles

An efficient route to α -methylene- γ -lactones involves the Ru-catalyzed [2+2+1] cycloadditions of allenyl aldehydes and ketones with CO (see scheme; $n = 1, 2$; $R = H, CH_3$; $X = NTs, O, C(CO_2Et)_2$; Ts = toluene-4-sulfonyl). The α -methylene- γ -lactone moiety is found in numerous biologically active natural products.



Angew. Chem. **2002**, *114*, 1654–1656

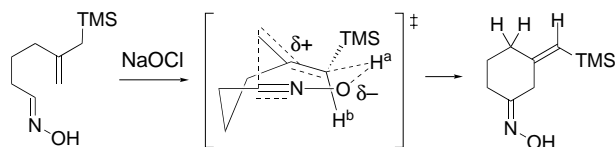
S.-K. Kang,* K.-J. Kim,
Y.-T. Hong 1584–1586

Synthesis of α -Methylene- γ -
butyrolactones: Ru-Catalyzed
Cyclocarbonylation of Allenyl Aldehydes
and Allenyl Ketones

Keywords: aldehydes • allenes •
cycloaddition • ketones • lactones •
ruthenium



“I took the road less traveled by and that has made all the difference.” Not only fans of the poet Robert Frost recognize the attraction of the less common reaction path. Rather than the expected [3+2] cycloaddition, a novel ene-like cycloisomerization occurs on deprotonation of allyltrimethylsilyl–oxime compounds when the β -sp² carbon atom of the allyltrimethylsilyl moiety is tethered to the oxime unit (see scheme). The resulting nitrile oxide functional group serves as an enophile, and the final cyclized product still has two functional groups suitable for further manipulations. TMS = SiMe₃.



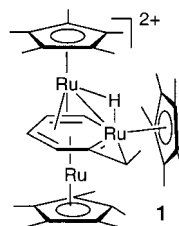
Angew. Chem. **2002**, *114*, 1656–1658

T. Ishikawa,* J. Urano, S. Ikeda,
Y. Kobayashi, S. Saito* 1586–1588

Novel Ene-Like Cycloisomerization
Reaction of Nitrile Oxides with a
Tethered Allyltrimethylsilyl Group

Keywords: cycloisomerization • nitrile
oxides • oximes • synthetic methods

Although their existence was suggested eight years ago, triple-decker complexes with a central metallabenzene have not been synthesized before. The ruthenabenzene-bridged complex **1** appears to be the first well-characterized example of a complex of this type with a bridging metallabenzene. The unusual central ligand was formed from coordinated norbornadiene via vinylcyclopentadiene.



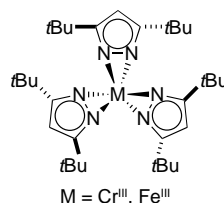
Angew. Chem. **2002**, *114*, 1659–1661

S. H. Liu, W. S. Ng, H. S. Chu, T. B. Wen,
H. Xia, Z. Y. Zhou, C. P. Lau,
G. Jia* 1589–1591

A Triple-Decker Complex with a Central
Metallabenzene

Keywords: C–C activation • coordination
chemistry • metallacycles • ruthenium •
sandwich complexes

η^2 coordination of pyrazolato ligands is currently unknown for d-block metal complexes with d² or higher electronic configurations, and all known Group 6–11 metal–pyrazolato complexes contain η^1 , μ : η^1 , η^1 , or η^5 ligands. Tris(3,5-di-*tert*-butylpyrazolato)chromium(III) and tris(3,5-di-*tert*-butylpyrazolato)iron(III) (see picture), which contain η^2 -pyrazolato ligands, have been synthesized, and molecular-orbital calculations indicate that η^2 -pyrazolato coordination is less stable than η^1 coordination in a model iron(III) complex.



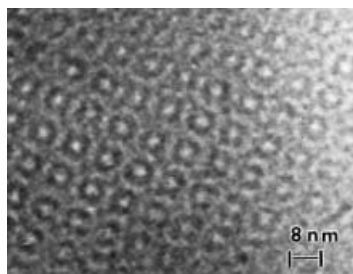
Angew. Chem. **2002**, *114*, 1661–1664

K. R. Gust, J. E. Knox, M. J. Heeg,
H. B. Schlegel,
C. H. Winter* 1591–1594

Synthesis, Structure, and Molecular
Orbital Calculations of Chromium(III) and
Iron(III) Complexes Containing
 η^2 -Pyrazolato Ligands

Keywords: ab initio calculations •
chromium • iron • ligand design •
N ligands

Acidic pores: The first cubic mesoporous tin(IV) phosphate and its hexagonal form are reported and characterized by X-ray diffraction, transmission electron microscopy (see picture of the cubic domain), and Brunauer–Emmet–Teller techniques. Microcalorimetric experiments and preliminary catalytic tests indicate that these solids are very acidic and exhibit a good catalytic activity for the removal of NO_x (deNO_x).



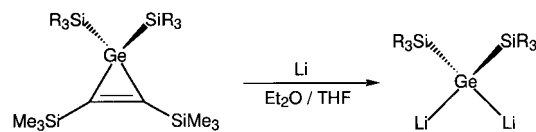
Angew. Chem. **2002**, *114*, 1664–1667

C. Serre,* A. Auroux, A. Gervasini,
M. Hervieu, G. Férey 1594–1597

Hexagonal and Cubic Thermally Stable
Mesoporous Tin(IV) Phosphates with
Acidic and Catalytic Properties

Keywords: heterogeneous catalysis •
mesoporous materials •
microcalorimetry • nitrogen oxides •
phosphates • tin

1,1-Dilithiogermaenes 1a and 1b were obtained by treatment of the persilyl-substituted germacycloprenes with lithium, which cleaved the two Ge–C bonds in the three-membered ring. The structure of **1b** has been confirmed by X-ray crystallography and shows a dimeric structure with a rather unusual arrangement of the two Li atoms. The use of **1** in the effective preparation of double-bonded derivatives of heavier Group 14 elements has also been shown.



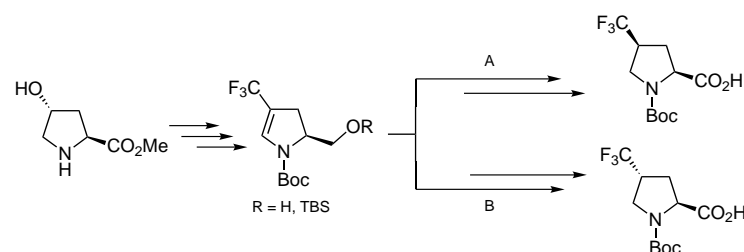
a: $R_3 = tPr_3$, **b:** $R_3 = tBu_2Me$

1

Angew. Chem. **2002**, *114*, 1668–1670



Stereocontrolled synthesis of *cis* and *trans*-substituted prolines by a divergent approach, leads to the preparation of *cis*-(4*S*)- and *trans*-(4*R*)-trifluoromethyl-L-proline from hydroxyproline. The key pyrroline intermediates were subjected to hydrogenation (see scheme; A = sterically directed hydrogenation, B = hydroxy-directed hydrogenation; Boc = *tert*-butoxycarbonyl, TBS = *tert*-butyldimethylsilyl), to afford products in high diastereomeric excess.



Angew. Chem. **2002**, *114*, 1670–1672



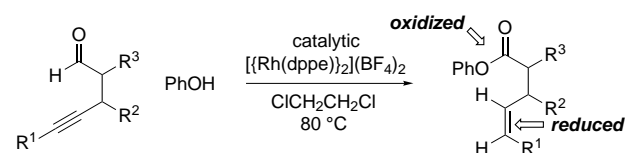
Can enzymes help organic chemists identify new transition-metal catalysts? The first example of the *in situ* enzymatic monitoring of an organic transformation is described. Thus, a transition-metal-mediated allylic-amination reaction in the organic layer (see scheme; $R = para$ -methoxyphenyl, tosyl) leads to release of ethanol which causes the spectroscopically observable formation of NADH in the aqueous phase. This approach uncovers a new Ni^0 -promoted route to β,γ -unsaturated amino acids. HMDS = 1,1,1,3,3,3-hexamethyldisilazane.



Angew. Chem. **2002**, *114*, 1673–1677



Two complementary transformations in one go: A rhodium-catalyzed transformation has been developed in which a phenol reacts with a 4-alkynal to furnish a *cis*-4-alkenoate in good yield (see scheme; dppe = 1,2-bis(diphenylphosphino)ethene). This novel tandem process couples the reduction of an alkyne to an alkene with the oxidation of an aldehyde to an ester.



Angew. Chem. **2002**, *114*, 1677–1679

A. Sekiguchi,* R. Izumi, S. Ihara,
M. Ichinohe, V. Y. Lee 1598–1600

The First Isolable 1,1-Dilithiogermaene and Its Unusual Dimeric Structure—An Effective Reagent for the Preparation of Double-Bonded Derivatives of Group 14 Elements

Keywords: alkali metals • germanium • lithium • reduction • small ring systems

J. R. Del Valle,
M. Goodman* 1600–1602

Stereoselective Synthesis of Boc-Protected *cis* and *trans*-4-Trifluoromethylprolines by Asymmetric Hydrogenation Reactions

Keywords: amino acids • diastereoselectivity • hydrogenation • peptidomimetics • trifluoromethylation

D. B. Berkowitz,* M. Bose,
S. Choi 1603–1607

In Situ Enzymatic Screening (ISES): A Tool for Catalyst Discovery and Reaction Development

Keywords: allylic substitution • amino acids • catalyst screening • enzymes • nickel • transition metals

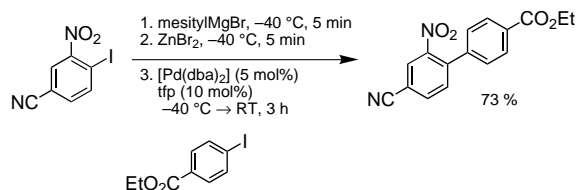
K. Tanaka, G. C. Fu* 1607–1609

A Novel Rhodium-Catalyzed Reduction–Oxidation Process: Reaction of 4-Alkynals with Phenol to Provide *cis*-4-Alkenoates

Keywords: alkynes • homogeneous catalysis • oxidation • reduction • rhodium



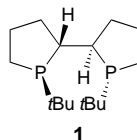
Highly functionalized aryl Grignard reagents with an *ortho*-nitro substituent have been synthesized from 2-iodonitroaryl compounds through an I–Mg exchange reaction with PhMgCl or mesityl magnesium bromide (see scheme). These reagents are stable ($T < -20^{\circ}\text{C}$ for several hours) and undergo various cross-coupling reactions in the presence of Cu or Pd catalysts (dba = *trans,trans*-dibenzylideneacetone; tfp = tri-*o*-furylphosphane).



Angew. Chem. **2002**, *114*, 1680–1681



TangPhos (1) is a highly efficient and practical ligand for asymmetric hydrogenations. High enantioselectivities and turnover numbers were observed in the Rh-catalyzed hydrogenation of α -(acylamino)acrylic acids and α -arylenamides.



Keywords: cross-coupling • Grignard reaction • halogen–magnesium exchange • iodine • nitro group

W. Tang, X. Zhang* 1612–1614

A Chiral 1,2-Bisphospholane Ligand with a Novel Structural Motif: Applications in Highly Enantioselective Rh-Catalyzed Hydrogenations

Keywords: asymmetric catalysis • enamides • hydrogenation • P ligands • rhodium

M. Reggelin,* M. Schultz, M. Holbach 1614–1617

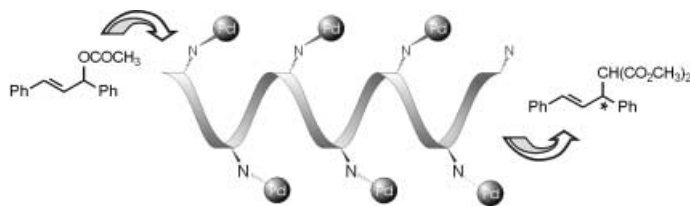
Helical Chiral Polymers without Additional Stereogenic Units: A New Class of Ligands in Asymmetric Catalysis

Keywords: allylic substitutions • asymmetric catalysis • chirality • helical structures • polymers

Angew. Chem. **2002**, *114*, 1682–1684



No other sources of chirality except its helicity are present in the polymeric ligand shown, which was prepared by helix-sense-selective polymerization. Palladium complexes of this ligand catalyze allylic substitution reactions. The resulting asymmetric induction is a direct and sole consequence of the uniform helicity of the polymeric ligand.



Angew. Chem. **2002**, *114*, 1684–1687



Supporting information on the WWW (see article for access details).



Accelerated publications

* Author to whom correspondence should be addressed

The cover picture was created with Macromodel/Maestro, WebLab Viewer Lite, and POV-Ray by Dr. Lubomir Sebo.



BOOKS

Handbook of Metalloproteins

Albrecht Messerschmidt,
Robert Huber, T. Poulos,
K. Wieghardt

F. Tucek 1619

Handbook of Nucleoside Synthesis

Helmut Vörbruggen,
Carmen Ruh-Pohlentz

P. Herdewijn 1620

Polyisoprenoids

Tanetoshi Koyama,
Alexander Steinbüchel

H. Lichtenthaler 1621

Flüchten, Mitmachen, Vergessen

Ute Deichmann

B. Schrader 1621

Solid Support Oligosaccharide Synthesis and Combinatorial Carbohydrate Libraries

Peter H. Seeberger

G. Drager, A. Kirschning 1622

Chiral Intermediates

Cynthia A. Challener

H. J. Martin 1623



SERVICE

• VIPs	1450	• Keywords	1626
• <i>Angewandte's</i> Sister-Journals	1461 – 1463	• Authors	1627
• Sources	A39	• Preview	1628
• Classifieds	A41		

Don't forget all the Tables of Contents
from 1998 onwards may be still found
on the WWW under:
<http://www.angewandte.com>

Issue 8, 2002 was published online on April 16.

CORRIGENDA

In the Communication by **A. Plückthun and G. M. Blackburn et al.** in Issue 5, **2002**, pp. 775–777 a footnote was not included, which points out that the authors J. R. Betley and S. Cesaro-Tadic contributed equally to this work. The editors apologize for the error.

In the Review by **S. J. Rowan et al.** in Issue 6, **2002**, pp. 898–952, an error was inadvertently introduced into Scheme 49 during the printing process. The correct scheme is shown below. The editorial team apologizes for this error.

